Available online at www.sciencedirect.com
ScienceDirect
Trans. Nonferrous Met. Soc. China 26(2016) 1975−1984
Transactions of Nonferrous Metals Society of China
www.tnmsc.cn

Dynamic experiments on flocculation and sedimentation of argillized ultrafine tailings using fly-ash-based magnetic coagulant

Shuai LI[1,2], Xin-min WANG[1,2], Qin-li ZHANG[1,2]

1. School of Resources and Safety Engineering, Central South University, Changsha 410083, China;
2. Key Laboratory of Mineral Resources Exploitation and Hazard Control for Deep Metal Mines, Central South University, Changsha 410083, China

Received 14 January 2016; accepted 6 June 2016

Abstract: In order to accelerate the sedimentation of super-large-scale argillized ultrafine tailings with bad features such as low settling velocity, muddy overflow water, and large flocculant dosage, a fly-ash-based magnetic coagulant (FAMC) was used in a dynamic experimental device. To obtain the best possible combination of the impact factors (magnetic intensity, FAMC dosage, flocculant dosage, and feed speed) for minimum overflow turbidity, a response surface methodology test coupled with a four-factor five-level central composite design was conducted. The synergy mechanism of FAMC and flocculant was analyzed based on the potential measurement and scanning electron microscopy. The results show that the flocculant dosage, overflow turbidity, and solid content can be reduced by 50%, 90%, and 80%, while the handling capacity per unit and efficiency of backfill and dry stacking can be promoted by 20%, 17%, and 13%, respectively, with a magnetic intensity of 0.3 T, FAMC dosage of 200 mL/t, flocculant dosage of 30 g/t, and feed speed of 0.6 t/(m^2·h). Therefore, synergy of FAMC and flocculant has obvious efficiency in saving energy and protecting the environment by allowing 70×10^6 t/a of argillized ultrafine tailings slurry to be disposed safely and efficiently with a cost saving of more than 53×10^6 Yuan/a, which gives it great promise for use in domestic and foreign mines.

Key words: super-large-scale argillized ultrafine tailings; flocculation and sedimentation; fly-ash-based magnetic coagulant; dynamic experimental device; response surface methodology; synergy mechanism

1 Introduction

There is now a general consensus that backfill and tailings dry stacking are ideal solutions for the safety of mining goafs and dealing with serious tailings pollutions on the surface [1,2]. As an important equipment of backfill and tailings dry stacking, deep-cone thickener is widely used to obtain high concentration underflow. By adding flocculants or coagulants, the settling velocity of fine tailings will be accelerated and the underflow concentration can be improved to 50%−60% [3]. The Sijiaying Iron Mine (Hebei Iron and Steel Group, China) is the biggest iron mine in Asia and produces more than 70×10^6 t of tailings slurry annually with a mass concentration of 20%. Due to the low-grade ore, serious argillation, and high oxidation, the super-large-scale argillized ultrafine tailings slurry is full of negatively charged slimes and ultrafine tailings (SUT). Like poles repel, and repulsive interactions of different particles lead to many problems such as low settling velocity and handling capacity per unit (HCPU), high overflow turbidity and solids content, and large flocculant dosage.

Flocculation and sedimentation of SUT include complex physical and chemical reactions [4]. SELOMULYA et al [5] used 3D tomographic imaging to predict the structure and permeability of flocculated structures and sediments directly. BÜRGERA et al [6] built a mathematical model for batch and continuous thickening of flocculated suspensions in vessels with varying cross-sections. FRANKS et al [7] conducted continuous solid–liquid separations with temperature-responsive flocculant N-isopropyl acrylamide, which produced higher concentration underflow but lower clarity overflow. ZHANG [8] designed a new test device using microorganisms, degradable modified polyacrylamide polymer flocculant st-PAM, and calcium chloride to make full use of high-performance polymer

Foundation item: Project (2012BAC09B02) supported by the 12th-Five Years Key Programs for Science and Technology Development of China; Project (2015zzts078) supported by the Fundamental Research Funds for the Central Universities of Central South University, China; Project (2015CX005) supported by Innovation Driven Plan of Central South University, China
Corresponding author: Shuai LI; Tel: +86-15200826420; E-mail: 15200826420@163.com
DOI: 10.1016/S1003-6326(16)64308-X

agent in coal slurry treatment. These researches provide an in-depth understanding of the flocculation and sedimentation of ultrafine particles. Nevertheless, advanced materials like temperature-responsive flocculant are still at the laboratory test stage, and the use of microorganisms in flocculation is a long-duration and complex work, so their widespread use at large scale cannot be afforded.

Magnetic separation, which is widely used in wastewater treatment and minerals separation, has shown great advantages in low investment, small area occupied, and short period of processing [9]. Magnetic seeds, which are added and uniformly mixed with the slurry previously, will adhere to the surface of diamagnetic particles and make them paramagnetic, and then sedimentation will be accelerated under the function of a magnetic field [10]. Fly ash is a solid waste residue of thermal power plants, with an annual output of 5×10^6 t all over the world [11,12]. However, the current recycling rate of fly ash is only 15%, and billion tons of untreated fly ash may cause serious environmental problems by polluting the water, atmosphere, soil, and landscape through dust generation [13]. Meanwhile, fly ash is rich in magnetic Fe_3O_4 [14], making it a rich resource and low-cost magnetic seed. Due to its various surface structures and potentially many chemically active points, fly ash needs to be modified by acid leaching for better contaction with SUT. Acid mine drainage (AMD), which typically contains high concentrations of dissolved heavy metals and low pH values, is an unavoidable byproduct of iron mines [15]. Instead of discharging AMD into public streams after a high investment and time-consuming treatment, recycling of AMD as acid-modified reagent for fly ash is economical and environmentally friendly.

On the basis of the above discussion, in this study, FAMC was prepared by leaching of fly ash in AMD. A response surface methodology (RSM) test coupled with a four-factor five-level central composite design (CCD) was conducted to obtain the best possible combination of the impact factors for minimum overflow turbidity. The synergy mechanism of FAMC and flocculant was analyzed based on zeta potential determination and scanning electron microscopy (SEM).

2 Experimental

2.1 Materials

As a typical of Anshan-type hematite mine, the tailings of Sijiaying have low loose density and high porosity; and the other main physical properties are shown in Table 1. The average particle size is only 19 μm, and more than 60% of the content is smaller than 20 μm, which is consistent with the composition requirements of ultrafine tailings. Because of the low-grade ore, serious argillation, and high oxidation, the tailings contain several argillaceous minerals like quartz, biotite, and chlorite. Various combinations of flocculants and coagulants with different dosages added were tested, while the overflow turbidity was still higher than 90 NTU. Table 2 presents the particle sizes (D) of SUT in overflow. More than 70% of the SUT is smaller than 6.7 μm and is covered by a strongly negatively charged thick hydration shell that blocks contact with flocculant. These ultrafine particles seem to have a stable colloform texture that makes flocculation and sedimentation difficult [16].

Table 1 Physical properties of tailings in Sijiaying

Density/ ($t\cdot m^{-3}$)	Loose density/ ($t\cdot m^{-3}$)	Average particle size/μm	Porosity/ %	Content of <20 μm/ %	Content of >74 μm/ %	pH
3.09	1.40	19	55.66	63.02	8.9	7−8

Table 2 Particle size of SUT in overflow

D/μm	Content/%
D>47	4.10
47>D>36	1.30
36>D>26	3.05
26>D>18	5.20
18>D>6.7	14.55
D< 6.7	71.8

Fly ash used in the study comes from the thermal power station in Tangshan, China, and its chemical composition is shown in Table 3. Because of abundant in magnetic Fe_3O_4 and active ingredient Al_2O_3, the fly ash is a suitable magnetic seed with strong magnetism and activity. However, the average particle size of the fly ash is only 50 μm, which is much bigger than that of the tailings. Therefore, the fly ash needs to be ground for better contact reaction and acid leached for potential active excitation.

Table 3 Chemical composition of fly ash (mass fraction, %)

SiO_2	Al_2O_3	Fe_2O_3	Fe_3O_4	CaO	MgO	TiO_2	Na_2O	SO_3
46.85	21.32	10.15	9.88	2.12	0.71	0.49	0.87	0.95

After being treated with sedimentation and filtration, the pH of AMD was 3.5. Due to the fact that the volume of AMD added to 1 t of tailings slurry for acid-leaching is only 200 mL, therefore, the negative effects of different concentrations of heavy metal ions and other impurities can be neglected. FAMC used in this study was prepared according to the following four steps.

1) Sieving

The impurities were eliminated and the fly ash was ground finely before being sieved in a 0.075 mm sieve.

2) Magnetic separation

The undersized fly ash was separated by a high-intensity magnetic separator for magnetic seeds, and the rest was recycled for filling material.

3) Grinding

The magnetic seeds were further ground to a size of less than 5 μm by a high-speed vibrating ball mill.

4) Acid leaching

The ground magnetic seeds were acid-leached to achieve a specific proportion ($m_{\text{fly ash}}/V_{\text{AMD}}$=1/2 g/mL), and then the acid-modified slurry was stirred for about 30 min to complete the full reaction.

2.2 Experimental apparatus

A self-made magnet coil was used to obtain a continuously adjustable magnetic intensity by controlling a DC electrical source. The magnetic intensity was measured by a Gauss meter (BST, China). A 2100Q turbidimeter (Hach, America) was used to measure the overflow turbidity, a JS94W zeta potential meter (Zykx, China) was used for the zeta potential test, and a S3500 laser particle analyzer (Microtrac, America) was used for particle size analysis.

The flocculation and sedimentation experiments were conducted in a further improved dynamic experimental device. Four peristaltic pumps were added to pump the tailings slurry, FAMC solution, flocculant solution, and underflow slurry, respectively. A feed trough at the top was designed to simulate the uniformly tangential type of feeding of the deep-cone thickener. The rake rod and harrow frame were designed to sample the overflow water and underflow slurry conveniently. The schematic diagram and working photograph are shown in Fig. 1.

Applications of the dynamic experimental device were as follows.

1) Tailings slurry was mixed with FAMC uniformly using an electric mixer in a 50 L mixing barrel. The mixed slurry was pumped to the feeding inlet with a concentration meter controlling the concentration.

2) Polyacrylamide (PAM) was selected as the flocculant after various combination tests. The PAM solution was configured in advance and then pumped into the feed trough in two different positions. Then, the DC electrical source was switched on and suitable magnetic intensity was provided by a self-made magnet coil.

3) The rotor was designed to guide the flow and extrude the pore water between tailings. The slow rotation speed (3−5 r/min) was controlled by a reduction motor.

2.3 Impact factors and evaluation index

In the synergy of FAMC and flocculant, the most important factors affecting the flocculation and sedimentation of tailings are the magnetic intensity, FAMC dosage, tailings concentration, feed speed, pH value, temperature, and PAM dosage [17,18]. Considering that Sijiaying produces more than 70×10^6 t of tailings slurry annually with a mass concentration of 20%, either attenuation or concentration is a huge project requiring heavy investment, the same as the adjustment of temperature. Besides, the tailings are neutral to slightly alkaline, which is suitable for PAM and FAMC working.

The most common evaluation indexes are the settling velocity, HCPU, underflow concentration, overflow turbidity, solids content, and so on. Considering that the tailings slurry in deep-cone thickener is in a relatively static state because of the supply and discharge balance, it is difficult to detect the settling velocity and HCPU with high accuracy. In addition, the solids content in overflow is about 5 g/L, which is much smaller than the underflow slurry density (about 2 kg/L), so it is also difficult to detect the underflow concentration and solids content in overflow accurately.

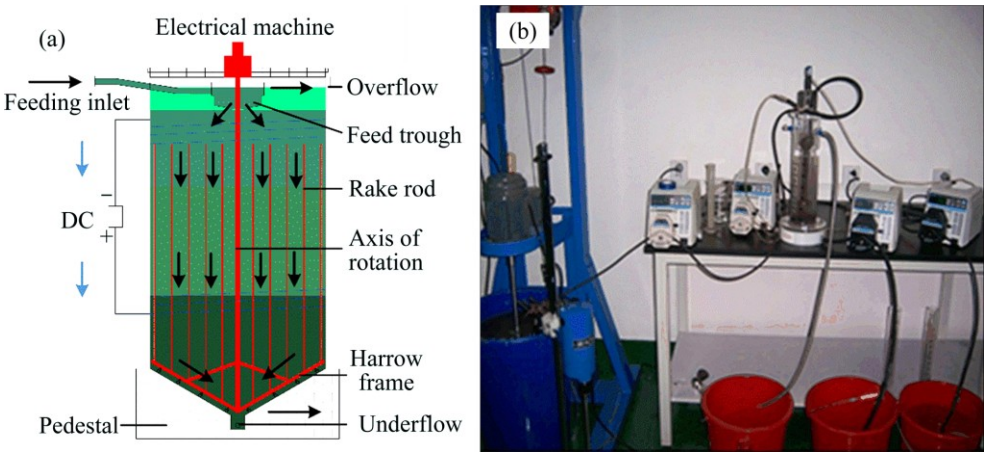

Fig. 1 Dynamic experimental device: (a) Schematic diagram; (b) Working photograph

In summary, the magnetic intensity, FAMC dosage, feed speed, and PAM dosage were taken as impact factors, and the overflow turbidity was selected as the evaluation index.

2.4 Experimental design

RSM is an important branch of the experimental design used in the development of new processes and optimization of their performance [19]. Through reasonable and effective experimental design, the relationships between impact factors and evaluation indexes were analyzed, and the optimum condition is found. To obtain the best possible combination of the four independent impact factors (X_1, magnetic intensity, 0−0.6 T; X_2, FAMC dosage, 0−400 mL/t; X_3, PAM dosage, 0−60 g/t; X_4, feed speed, 0.2−1.0 t/(m^2·h) for minimum overflow turbidity, an RSM test coupled with a four-factor five-level CCD was conducted using Design Expert 8.0.5b. The working ranges of impact factors are shown in Table 4. The experimental design consisted of

Table 4 Working ranges of impact factors

Symbol	Process parameter	Notation	Level coded				
			−2	−1	0	+1	+2
1	Magnetic intensity/T	X_1	0	0.15	0.30	0.45	0.60
2	FAMC dosage/(mL·t^{-1})	X_2	0	100	200	300	400
3	PAM dosage/(g·t^{-1})	X_3	0	15	30	45	60
4	Feed speed/(t·m^{-2}·h^{-1})	X_4	0.2	0.4	0.6	0.8	1.0

Table 5 Design of experiments and responses

Run	Point type	Magnetic intensity X_1/T	FAMC dosage X_2/(mL·t^{-1})	PAM dosage X_3/(g·t^{-1})	Feed speed X_4/(t·m^{-2}·h^{-1})	Turbidity Y/10^{-6}
1	Factorial	0.15	100	15	0.4	37.9
2	Factorial	0.45	100	15	0.4	21.1
3	Factorial	0.15	300	15	0.4	42.4
4	Factorial	0.45	300	15	0.4	31.0
5	Factorial	0.15	100	45	0.4	18.7
6	Factorial	0.45	100	45	0.4	13.2
7	Factorial	0.15	300	45	0.4	22.7
8	Factorial	0.45	300	45	0.4	16.3
9	Factorial	0.15	100	15	0.8	94.5
10	Factorial	0.45	100	15	0.8	79.4
11	Factorial	0.15	300	15	0.8	81.8
12	Factorial	0.45	300	15	0.8	52.8
13	Factorial	0.15	100	45	0.8	57.9
14	Factorial	0.45	100	45	0.8	41.7
15	Factorial	0.15	300	45	0.8	37.2
16	Factorial	0.45	300	45	0.8	11.4
17	Axial	0.00	200	30	0.6	90.3
18	Axial	0.60	200	30	0.6	13.7
19	Axial	0.30	0	30	0.6	94.3
20	Axial	0.30	400	30	0.6	32.0
21	Axial	0.30	200	0	0.6	156
22	Axial	0.30	200	60	0.6	10.1
23	Axial	0.30	200	30	0.2	9.80
24	Axial	0.30	200	30	1.0	119
25	Center	0.30	200	30	0.6	10.6
26	Center	0.30	200	30	0.6	9.89
27	Center	0.30	200	30	0.6	10.1
28	Center	0.30	200	30	0.6	10.3
29	Center	0.30	200	30	0.6	9.71
30	Center	0.30	200	30	0.6	9.43

30 runs, which are listed in Table 5. A flowchart summarizing the whole experimental program is displayed in Fig. 2.

3 Results and analysis

3.1 Experimental design analysis

Various mathematical models were introduced to obtain the regression equations. The model summary statistics (Table 6) were determined to select the best model, that is, the model that exhibits the highest R^2, adjusted R^2, predicted R^2 and F values, and the lowest p-values when compared with those of the other models [20]. Thus, the quadratic model was selected for further analysis, and the obtained second-order polynomial equations is given below:

$$Y=137.28-191.13X_1-0.19X_2-3.97X_3-27.30X_4-0.08X_1X_2+0.51X_1X_3-95.83X_1X_4-0.0008X_2X_3-0.35X_2X_4-2.01X_3X_4+285.87X_1^2+0.0009X_2^2+0.06X_3^2+283.30X_4^2$$

A diagnostic plot of predicted versus actual values (Fig. 3) was created to evaluate the model suitability and accuracy. The data points on the plot lie reasonably close to a straight line, which indicates an adequate agreement between the real data and the data obtained from the model [21]. Pareto analysis of variance (ANOVA) was employed to evaluate the statistical significance of the regression equation, and the results are presented in Table 7. The model F value of 4.68 implies that the model is significant and there is only 0.26% chance that a large model F value could occur due to noise. Values of "Prob>F" less than 0.0500 indicate that the model terms are significant, and X_1, X_3, X_4, X_3^2, and X_4^2 are significant model terms in this case. These results indicate that the developed mathematics is good enough to represent the relationship between impact factors and evaluation index [22].

3.2 Effect of magnetic intensity and FAMC dosage

For a PAM dosage of 30 g/t and a feed speed of 0.6 t/(m^2·h), the response surface plot and contour plot of magnetic intensity and FAMC dosage are shown in Fig. 4. We defined X_1 and X_2 as zero as there was no effect of magnetic field when the overflow turbidity was set at a high value of 100 NTU. This proves that flocculation and sedimentation of SUT under the action of a single flocculant are difficult. When magnetization was applied, SUT settled quickly, leading to a rapid decline in overflow turbidity. The peak occurred at X_1 as 0.3 T and X_2 as 200 mL/t, when the turbidity declined by 92% to 10 NTU. The turbidity rose gradually while X_1 and X_2 continued to increase.

3.3 Effect of magnetic intensity and PAM dosage

For a FAMC dosage of 200 mL/t and a feed speed of 0.6 t/(m^2·h), the response surface plot and contour plot of magnetic intensity and PAM dosage are shown in Fig. 5. We defined X_3 as zero as there was no effect of the flocculant when the overflow turbidity was set at a

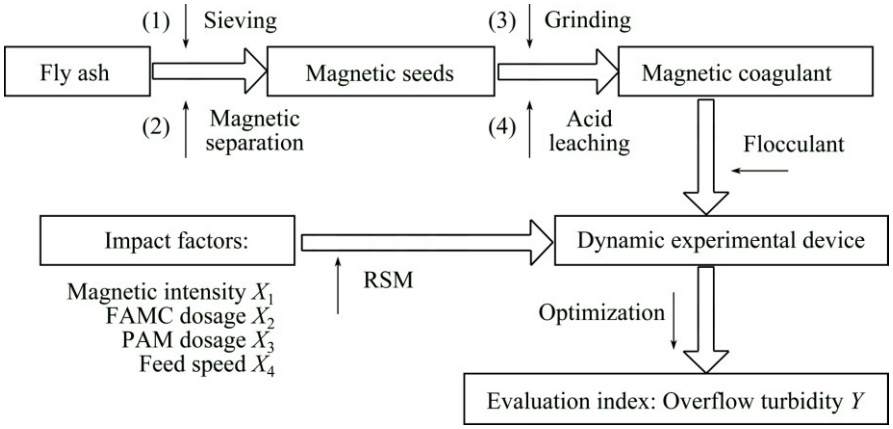

Fig. 2 Flowchart of whole experimental program

Table 6 Model summary statistics

Source	SD	R^2	Adjusted R^2	Predicted R^2	Press	Remark
Linear	26.873991	0.5813975	0.5144211	0.413913	25279.273	−
2FI	29.438121	0.6182568	0.4173394	0.318084	29412.598	−
Quadratic	23.135156	0.8138626	0.6401344	–0.072063	46240.537	Suggested
Cubic	21.324556	0.9262001	0.6942577	–9.624268	458248.99	Aliased

SD—Standard deviation; 2FI—2 function interaction

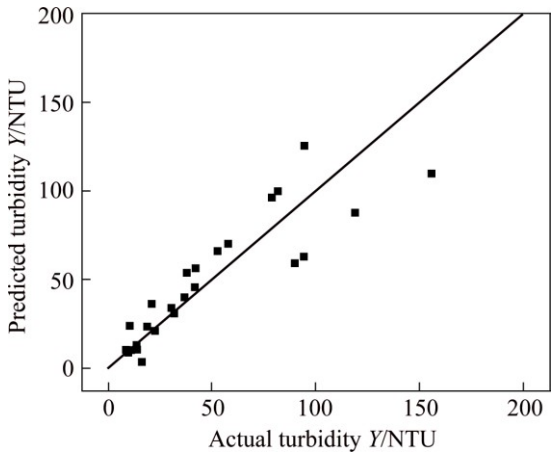

Fig. 3 Plot of actual versus predicted turbidity

Table 7 Analysis of variance of central composite design

Source of variation	Sum of squares	Degree of freedom	Mean square	*F* value	Prob>*F*
Model	35103.758	14	2507.4113	4.6846883	0.0026
X_1	3252.6817	1	3252.6817	6.0771043	0.0262
X_2	1558.4817	1	1558.4817	2.9117684	0.1085
X_3	10991.04	1	10991.04	20.534963	0.0004
X_4	9274.8017	1	9274.8017	17.328452	0.0008
X_1X_2	22.5625	1	22.5625	0.0421543	0.8401
X_1X_3	21.16	1	21.16	0.039534	0.8451
X_1X_4	132.25	1	132.25	0.2470875	0.6263
X_2X_3	22.5625	1	22.5625	0.0421543	0.8401
X_2X_4	781.2025	1	781.2025	1.4595492	0.2457
X_3X_4	610.09	1	610.09	1.1398535	0.3026
X_1^2	1134.7665	1	1134.7665	2.1201259	0.1660
X_2^2	2331.4482	1	2331.4482	4.3559301	0.0544
X_3^2	5526.4785	1	5526.4785	10.325322	0.0058
X_4^2	2492.1768	1	2492.1768	4.6562252	0.0476
Residual	8028.5318	15	535.23545		
Lack of fit	8027.6508	10	802.76508	4556.2466	< 0.0001
Pure error	0.88095	5	0.17619		
Total	43132.289	29			

high value of 156 NTU, which proves that FAMC has no effects on flocculation of SUT without flocculant. When PAM was added, SUT settled quickly under the synergy of FAMC and flocculant, leading to a rapid decline in overflow turbidity. The peak occurred at X_1 as 0.3 T and X_3 as 30 g/t, when the turbidity declined by 93% to 10 NTU. If PAM was constantly added, the costs rose quickly while the decrease of turbidity was inconspicuous.

3.4 Effect of PAM dosage and feed speed

For a magnetic intensity of 0.3 T and a FAMC dosage of 200 mL/t, the response surface plot and contour plot of PAM dosage and feed speed are shown in Fig. 6. When the feed speed was below 0.5 t/(m^2·h), the synergy of FAMC and flocculant was in a surplus condition, SUT settled quickly with a PAM dosage of 30 g/t, and the turbidity was below 10 NTU. When the feed speed exceeded 0.7 t/(m^2·h), the synergy of FAMC and flocculant was insufficient, and the overflow turbidity remained at more than 30 NTU although a large PAM dosage was added.

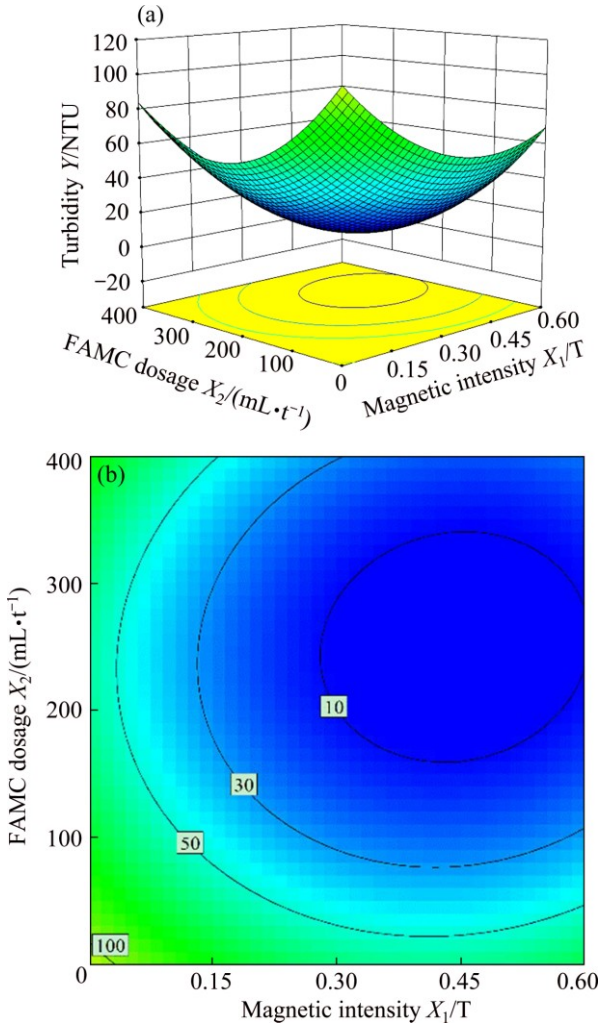

Fig. 4 Plots between magnetic intensity and FAMC dosage: (a) Response surface plot; (b) Contour plot

4 Mechanism and application

4.1 Synergy mechanism of FAMC and flocculant

With the progress of science and technology, better precision of potential measurements and SEM, X-ray diffraction and infrared spectra have been used to analyze the synergistic mechanism of FAMC and flocculant [23].

Being covered with strong negative charges, SUT will attract polarity water molecules nearby and form

thick hydration shells that blocks contact with PAM. Unlike traditional flocculants and coagulants, FAMC is rich in ground magnetic Fe_3O_4 and cations (Fe^{3+} and Al^{3+}). As we can see from Fig. 7, strong negative charges are neutralized by Fe^{3+} and Al^{3+}, which will lead to weaker repulsive interactions, thinner hydration shells and lower zeta potentials. As evidence, zeta potential of the overflow water before and after magnetization are 34.1 and 22.6 mV, respectively. Besides, ground magnetic seeds will attach to the surface of SUT uniformly, changing the particles from diamagnetic to paramagnetic. The paramagnetic particles can be magnetized into magnetic dipoles quickly by a magnetic field; then they undergo mutual attraction, gather, captured by PAM, and settle rapidly. According to the microstructures of flocs, the average particle size of flocs with PAM and FAMC added is about 380 μm, which is twice of the PAM flocs'. However, excessive magnetic

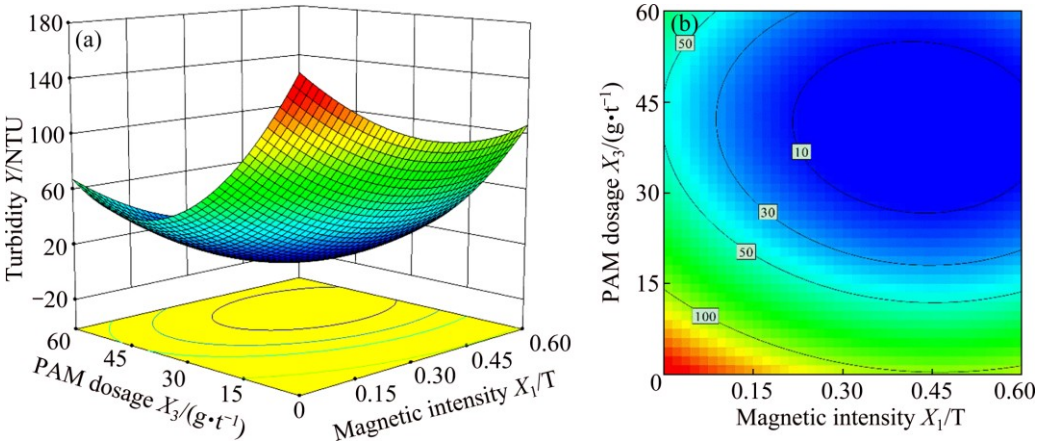

Fig. 5 Plots between magnetic intensity and PAM dosage: (a) Response surface plot; (b) Contour plot

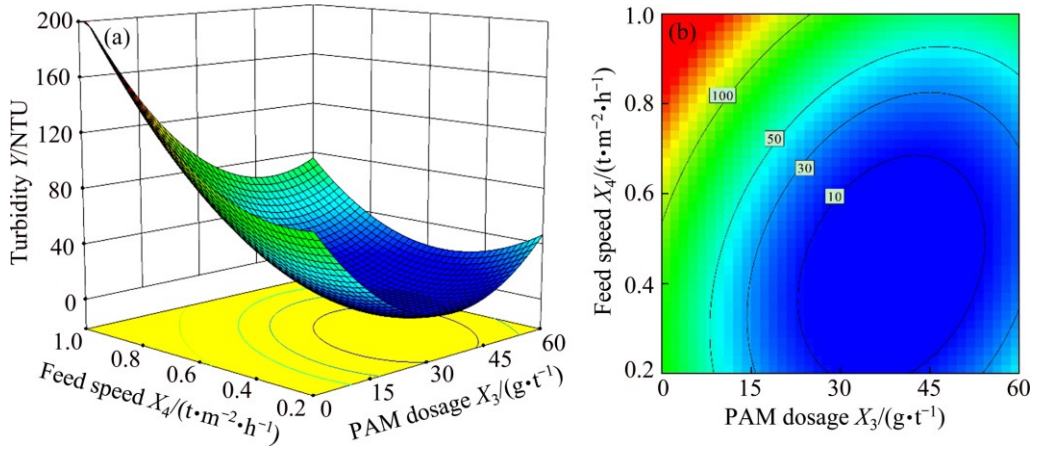

Fig. 6 Plots between PAM dosage and feed speed: (a) Response surface plot; (b) Contour plot

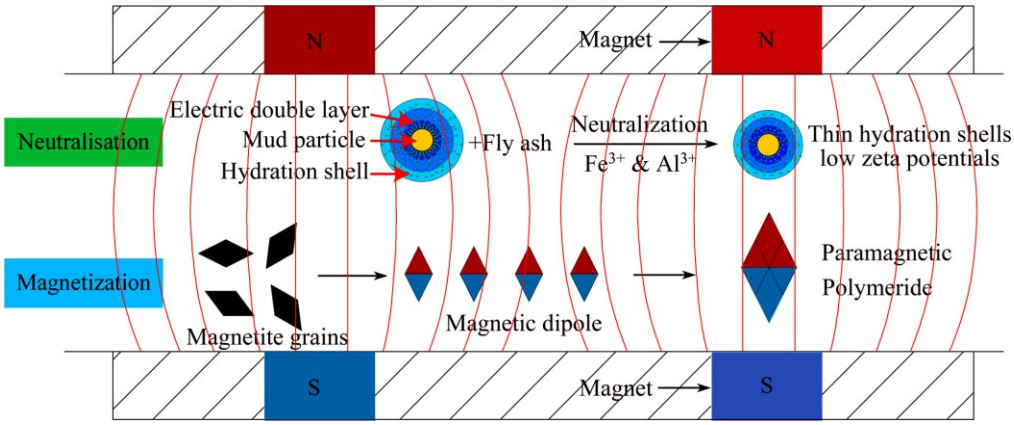

Fig. 7 Synergy mechanism of FAMC and flocculant

intensity and FAMC dosage will make the magnetic Fe_3O_4 settle too quickly to achieve a full contact reaction with SUT.

In view of energy, magnetic field provides continuous activation energy for flocculation and sedimentation of SUT. Physical and chemical reactions of flocculant molecules are sped up because the thermal motion of the magnetized water molecules increases and the viscosity decreases [24]. Comparison of SEM images between normal backfilling and magnetized backfilling with 10000× magnification after samples were kept in the laboratory for 28 d is shown in Fig. 8. Magnetized backfilling is more intact in structure and homogeneous in grain composition, which means that the sedimentation of SUT is more complete under the synergy of FAMC and flocculant.

4.2 Application effects

According to repeated tests, the optimal magnetizing conditions for flocculation and sedimentation of SUT in Sijiaying are a slurry mass concentration of 20%, magnetic intensity of 0.3 T, FAMC dosage of 200 mL/t, PAM dosage of 30 g/t, and feed speed of 0.6 t/(m^2·h). A comparison of the main parameter indexes before and after the use of FAMC can be seen in Table 8. Under the synergy of FAMC and flocculant, the PAM dosage, overflow turbidity, and solid content can be reduced by 50%, 90%, and 80%, respectively, while HCPU and the efficiency of backfill and dry stacking can be promoted by 20%, 17%, and 13%, respectively.

The use of FAMC is economical and environmentally friendly. Firstly, it can reduce costs by 53 million Yuan per year (see Fig. 9), while the PAM dosage can be reduced by more than 2100 t/a, which will save 63 million Yuan. Besides, more than 14000 t of AMD and 70000 t of fly ash are used annually for preparing the FAMC instead of polluting the

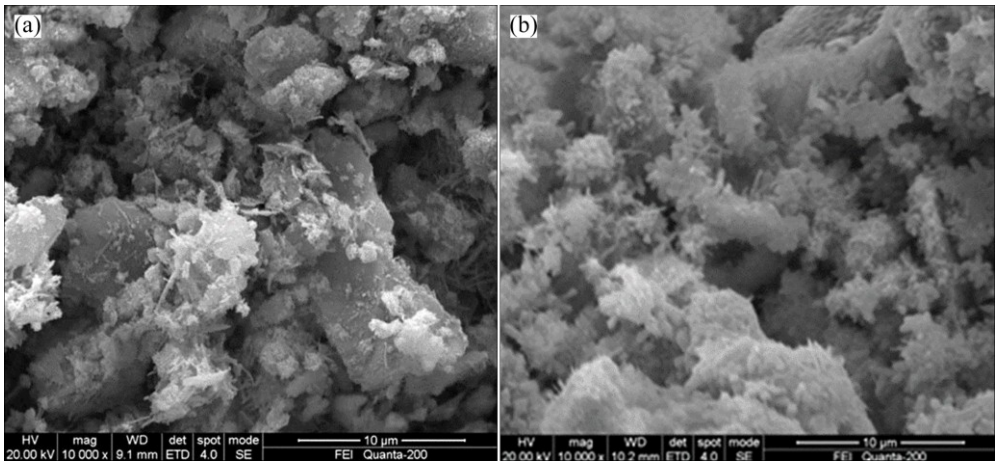

Fig. 8 Comparison of SEM images: (a) Normal backfilling; (b) Magnetized backfilling

Table 8 Comparison of main parameter indexes before and after use of FAMC

Parameter index	HCPU/ (t·m^{-2}·h^{-1})	PAM dosage/ (g·t^{-1})	Turbidity/ NTU	SCOW/ 10^{-6}	Backfill/ (m^3·h^{-1})	Dry stacking/ (kt·d^{-1})
PAM only	0.5	60	95	1500	180	22
FAMC and PAM	0.6	30	10	300	210	25

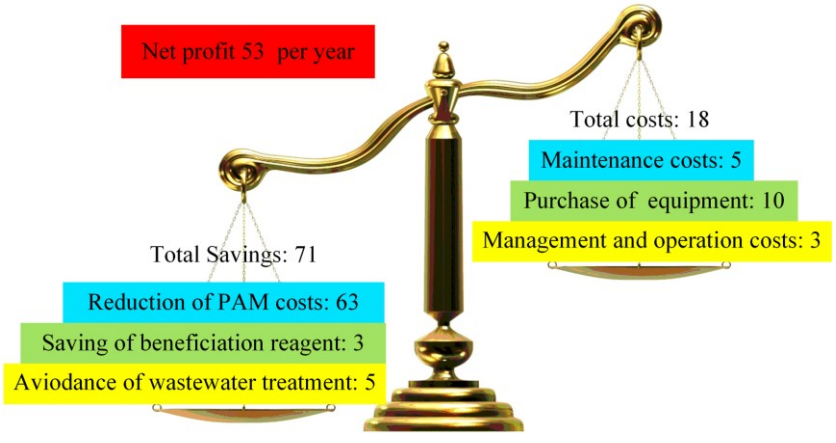

Fig. 9 Economic evaluation of use of FAMC (Unit: million Yuan)

environment. The overflow water can be used for beneficiation without treatment, which will save the costs of wastewater treatment and reduce the beneficiation reagent dosage at the same time. In addition, the efficiency of backfill and dry stacking can be promoted, reducing the consumption of electricity and energy for equipment effectively.

5 Conclusions

1) AMD and fly ash were used for preparing the FAMC instead of polluting the environment. An automatically controlled dynamic experimental device was designed to simulate the sedimentation mechanism of deep-cone thickener to the greatest extent. RSM test was conducted to obtain the best possible combination of the impact factors for minimum overflow turbidity, and the synergy mechanism of FAMC and flocculant was analyzed.

2) FAMC had no effect on flocculation of SUT without flocculant. Under the synergy of FAMC and flocculant, the turbidity declined rapidly as the magnetic intensity and FAMC dosage increased. However, excessive magnetic intensity and FAMC dosage made the magnetic Fe_3O_4 settle too quickly to achieve a full contact reaction with SUT.

3) By adding FAMC, the strong negative charges are neutralized by Fe^{3+} and Al^{3+}, leading to the zeta potential falls from 34.1 to 22.6 mV. Ground magnetic seeds attach to the surface of SUT uniformly, changing them from diamagnetic to paramagnetic, and they then undergo mutual attraction, gather, are caught by PAM, and settle rapidly.

4) The optimal magnetizing conditions are a magnetic intensity of 0.3 T, FAMC of 200 mL/t, PAM dosage of 30 g/t, and feed speed of 0.6 t/(m^2·h), at which the PAM dosage, overflow turbidity, and solid content can be reduced by 50%, 90%, and 80% while the HCPU and the efficiency of backfill and dry stacking can be promoted by 20%, 17%, and 13%, respectively.

References

[1] STICKLAND A D, REES C A, MOSSE K P, DIXON D R, SCALES P J. Dry stacking of wastewater treatment sludges [J]. Water Research, 2013, 47(10): 3534−3542.

[2] RULYOV N N, LASKOWSKI J S, CONCHA F. The use of ultra-flocculation in optimization of the experimental flocculation procedures [J]. Physicochemical Problems of Mineral Processing, 2011, 47: 5−16.

[3] WANG C, HARBOTTLE D, LIU Q, XU Z. Current state of fine mineral tailings treatment: A critical review on theory and practice [J]. Minerals Engineering, 2014, 58: 113−131.

[4] ADDAIMENSAH J. Enhanced flocculation and dewatering of clay mineral dispersions [J]. Powder Technology, 2007, 179(1): 73−78.

[5] SELOMULYA C, JIA X, WILLIAMS R A. Direct prediction of structure and permeability of flocculated structures and sediments using 3D tomographic imaging [J]. Chemical Engineering Research and Design, 2005, 83(7): 844−852.

[6] BÜRGER R, DAMASCENO J J R, KARLSEN K H. A mathematical model for batch and continuous thickening of flocculent suspensions in vessels with varying section [J]. International Journal of Mineral Processing, 2004, 73(2): 183−208.

[7] FRANKS G V, O'SHEA J P, FORBES E. Controlling thickener underflow rheology using a temperature responsive flocculant [J]. AIChE Journal, 2014, 60(8): 2940−2948.

[8] ZHANG Y J. Basic research on coal slurry advanced treatment by chemical and microbiological collaborative method [D]. Xuzhou: China University of Mining and Technology, China, 2014. (in Chinese)

[9] WANG S, STILES A R, GUO C, LIU C. Harvesting microalgae by magnetic separation: A review [J]. Algal Research, 2015, 9: 178−185.

[10] ZHAO Y, XI B, LI Y, WANG M, ZHU Z, XIA X, ZHANG L, WANG L, LUAN Z. Removal of phosphate from wastewater by using open gradient superconducting magnetic separation as pretreatment for high gradient superconducting magnetic separation [J]. Separation and Purification Technology, 2012, 86: 255−261.

[11] KAITHWAS A, PRASAD M, KULSHRESHTHA A, VERMA S. Industrial wastes derived solid adsorbents for CO_2 capture: A mini review [J]. Chemical Engineering Research and Design, 2012, 90(10): 1632−1641.

[12] OHENE ADU R, LOHMUELLER R. The use of organic waste as an eco-efficient energy source in ghana [J]. Journal of Environmental Protection, 2012, 3(7): 553−562.

[13] AHMARUZZAMAN M. A review on the utilization of fly ash [J]. Progress in Energy and Combustion Science, 2010, 36(3): 327−363.

[14] ZHOU Q, YAN C, LUO W. Polypyrrole coated secondary fly ash–iron composites: Novel floatable magnetic adsorbents for the removal of chromium (VI) from wastewater [J]. Materials & Design, 2016, 92: 701−709.

[15] PETRILAKOVA A, BALINTOVA M, HOLUB M. Precipitation of heavy metals from acid mine drainage and their geochemical modeling [J]. Selected Scientific Papers Journal of Civil Engineering, 2014, 9(1): 79−86.

[16] CHENG L, YU Y Z, ZHOU Y X, ZHANG H D, LI M W. The research progress of flocculants in sewage sludge dewatering [J]. Advanced Materials Research, 2012, 610: 1518−1521.

[17] ALAMGIR A, HARBOTTLE D, MASLIYAH J, XU Z. Al-PAM assisted filtration system for abatement of mature fine tailings [J]. Chemical Engineering Science, 2012, 80: 91−99.

[18] ALAM N, OZDEMIR O, HAMPTON M A, NGUYEN A V. Dewatering of coal plant tailings: Flocculation followed by filtration [J]. Fuel, 2011, 90(1): 26−35.

[19] MADADI F, ASHRAFIZADEH F, SHAMANIAN M. Optimization of pulsed TIG cladding process of stellite alloy on carbon steel using RSM [J]. Journal of Alloys and Compounds, 2012, 510(1): 71−77.

[20] THIRUGNANASAMBANDHAM K, SIVAKUMAR V, PRAKASH M J. Optimization of electrocoagulation process to treat biologically pretreated bagasse effluent [J]. Journal of the Serbian Chemical Society, 2014, 79(5): 613−626.

[21] MARAN J P, MANIKANDAN S, THIRUGNANASAMBANDHAM K, NIVETHA C V, DINESH R. Box–Behnken design based statistical modeling for ultrasound-assisted extraction of corn silk polysaccharide [J]. Carbohydrate Polymers, 2013, 92(1): 604−611.

[22] HSU M, JU T L, YEN C, CHANG C. Knowledge sharing behavior in virtual communities: The relationship between trust, self-efficacy, and outcome expectations [J]. International Journal of Human-Computer Studies, 2007, 65(2): 153−169.

[23] SANCHES E A, CAROLINO A D S, SANTOS A L D, FERNANDES E G R, TRICHÊS D M, MASCARENHAS Y P. The use of le bail method to analyze the semicrystalline pattern of a nanocomposite based on polyaniline emeraldine-salt form and α-Al_2O_3 [J]. Advances in Materials Science and Engineering, 2015, 2015: 1−8.

[24] BYRNE J M, COKER V S, CESPEDES E, WINCOTT P L, VAUGHAN D J, PATTRICK R A, TELLING N D. Biosynthesis of zinc substituted magnetite nanoparticles with enhanced magnetic properties [J]. Advanced Functional Materials, 2014, 24(17): 2518−2529.

基于新型磁化助凝剂的超细泥化全尾砂动态絮凝沉降实验

李 帅[1,2]，王新民[1,2]，张钦礼[1,2]

1. 中南大学 资源与安全工程学院，长沙 410083；
2. 中南大学 深部金属矿床开发与灾害控制重点实验室，长沙 410083

摘 要：为解决司家营铁矿超大规模超细泥化全尾砂浆体沉降速度慢、溢流水浑浊、絮凝剂单耗高等问题，基于新型磁化助凝剂，进行了室内超细泥化全尾砂动态絮凝沉降实验。为获得各影响因子(磁场强度、助凝剂单耗、絮凝剂单耗和供料速度)作用下最小的溢流水浊度，基于响应面分析法，进行了四因素五水平的中心组合实验设计。采用电位分析和电镜扫描等方法分析了助凝剂和絮凝剂的协同作用机理。结果表明：在磁场强度为 0.3 T，助凝剂单耗为 200 mL/t，絮凝剂单耗为 30 g/t，供料速度为 0.6 t/(m^2·h)时，絮凝剂单耗、溢流水浊度和含固量分别降低约 50%、90%和 80%；深锥单位面积处理能力、充填和干排效率分别提升约 20%、17%和 13%。新型磁化絮凝剂经济环保，在实现司家营铁矿 7000 万吨超细全尾砂浆体安全高效处置的基础上，可节约经济成本 5300 万元，在国内外矿山具有巨大的推广应用价值。

关键词：超细泥化全尾砂；絮凝沉降；磁化助凝剂；动态沉降实验；响应面分析法；协同作用机理

(Edited by Xiang-qun LI)